Angular Orientation of the Retinyl Chromophore of Bacteriorhodopsin: Reconciliation of ^{2}H NMR and Optical Measurements

Bruce S. Hudson[†] **and Robert R. Birge***

Department of Chemistry, Syracuse University, Syracuse, New York 13244-4100

Received: September 3, 1998; In Final Form: December 8, 1998

It is argued on the basis of MNDO−PSDCI calculations that, at the wavelength of electronic dichroism studies used to infer structure, the transition dipole moment of the retinyl Schiff's base chromophore of bacteriorhodopsin makes an angle of 10.5 ± 3.5° with respect to the long axis of the chromophore. The magnitude and direction of this off-axis angle helps to reconcile the differences between the deuterium NMR and optical determinations of the angular orientation of the chromophore in bacteriorhodopsin. Reconciliation of the NMR and optical dichroism structures is only possible, however, when the chromophore is oriented so that the imine proton points toward the extracellular surface. After correction, the published electronic dichroism data predict a chromophore angle of $\Omega = 61 \pm 7°$, where Ω is defined as the angle of a line connecting chromophore atoms C_5 and C_{15} relative to the membrane normal. The corresponding NMR results are $\Omega = 53.7 \pm 4.1°$. The combined data with equal weighting yield $\Omega = 57 \pm 8°$. This estimate is smaller than $\Omega = 70.6 \pm 3.2°$ derived from recent diffraction studies, and the possible origins of these differences are discussed.

Bacteriorhodopsin, the light-transducing proton pump in the purple membrane of *Halobacterium salinarium*, is configured in the membrane based on a 3-fold symmetric trimeric structure with the retinyl chromophore of each protein monomer oriented at an angle of $\Omega = 50-75°$ with respect to the membrane normal. In previous studies, the angular structure of the chromophore has been determined by using deuterium NMR[1−3] and several optical methods involving electronic[4−7] and vibrational[8,9] transitions. The more recent deuterium NMR studies[1,3] use CD_3 deuterated methyl groups at positions 18, 19, and 20 in the retinyl chain (see Figure 1). The precise value of the orientation of the CD_3 groups with respect to the bilayer normal depends on the specific methyl group. Given that each methyl group is expected to be normal to the local polyene chain, the average angle of tilt of the polyene chain determined by this method is $\Omega = 54°$ relative to the membrane normal.

The dichroism of the electronic absorption spectrum has also been used to determine this orientational angle. The early dichroism studies of Heyn, Cherry, and Müller obtained angles of $\Omega = 78 \pm 3°$ based on transient dichroism measurements and $\Omega = 71 \pm 4°$ based on linear dichroism measurements.[4] More recent electronic dichroism studies[5−7] measure values of $\Omega = 69°-70°$ (ref 5), $\Omega = 69°$ (ref 6), and $\Omega = 70.3°$ (ref 7). All of the experimental data are consistent within the range $\Omega = 71.5 \pm 7°$. This angle (rounded) is also shown in Figure 1. While one might consider the NMR and optical measurements to be in reasonable agreement, angular measurements of this type are usually more accurate. The ^{2}H NMR results are believed to be accurate to about 1°. In an earlier study[2] based on ^{2}H NMR using deuterated methyl groups in the β-ionone ring, a curvature of the retinyl chain was proposed to explain the difference between the orientation determined by the optical and NMR results. The more recent and extensive side chain deutero methyl results show that while there is apparently a bend to the polyene chain, the two sets of measurements can no longer be reconciled by introduction of any further chain bending since this is now proscribed by the data.

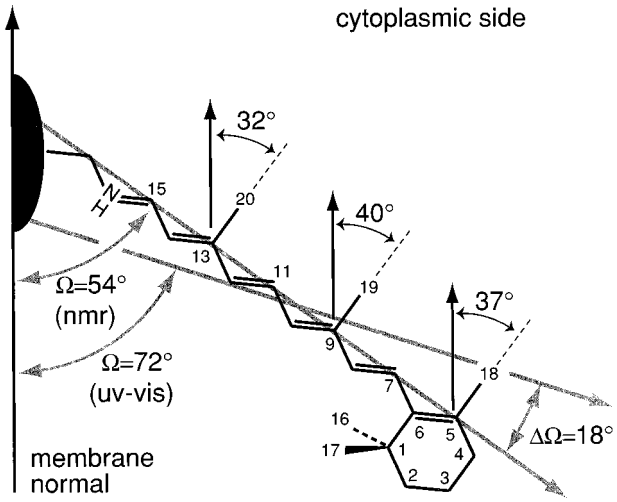

Figure 1. Orientation of the retinal chromophore relative to the membrane normal as determined from the average methyl group orientation, assuming that the methyl groups at positions 18−20 are perpendicular to the polyene chain compared to the transition dipole orientation determined from optical dichroism studies.

Another possibility noted in earlier studies[2] is that the source of this discrepancy stems from the assumption that the average chain axis of the retinyl polyene chain is coincident with the electronic transition moment. Support for this possibility derived from the observation[10] that for a simple alkyl substituted tetraene the off-axis angle has been shown to be 20° in a condensed-phase environment. In this paper, we discuss the possible origin for the ∼18° difference in the ^{2}H NMR and optical determinations of the average chain tilt angle of the retinal chromophore of bacteriorhodopsin (BR).

In a recent study in this issue,[11] we have reviewed the experimental work bearing on the off-axis angle for simple

[†] E-mail: bshudson@syr.edu.
* Corresponding author. E-mail: rbirge@syr.edu.

10.1021/jp9836271 CCC: $18.00
Published on Web 03/02/1999

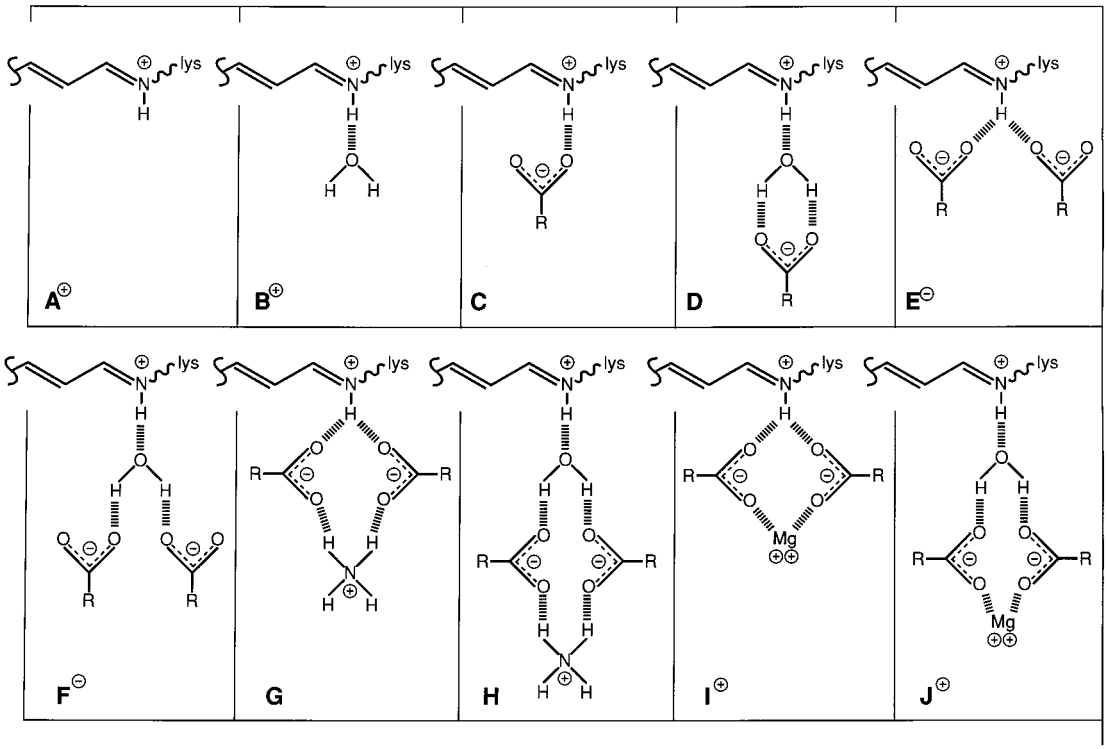

Figure 2. Model structures used for determination of the effect of the counterion and hydrogen bonding environment on the excitation energy and transition dipole orientation of the two lowest energy transitions of the retinal protonated Schiff's base.

polyenes[10,12−14] and have compared these experimental results with the results of semiempirical molecular orbital calculations. It was shown that properly parametrized[15,25] MNDO−PSDCI calculations are capable of predicting this off-axis angle with good accuracy.[11] Here we apply this same methodology to an analysis of the chromophore orientation in light-adapted bacteriorhodopsin.

Extra complications arise in this case because the chromophore of bacteriorhodopsin is a protonated Schiff's base. This significant substitution, which reverses the $2A_g/1B_u$ excited state ordering of symmetric polyenes, is likely to result in a significant change in the dipole orientation. The second interesting issue is the possible influence of the counterion and other secondary interactions such as hydrogen bonding of the Schiff's base proton on the transition dipole orientation. Finally, it must be born in mind that the lower symmetry of the protonated Schiff's base results in significant intensity in the "$2A_g$-like" state that has extensive double excitation character. This state is known from two-photon studies to lie slightly higher in energy than the "$1B_u$-like" state in bacteriorhodopsin (see discussion below). The transition dipole orientation of these two transitions might have different orientations relative to the molecular axis system.

Methods and Results

Ground-state minimizations of the binding site models examined were carried out by using MNDO/PM3 all-valence electron semiempirical molecular orbital procedures.[15−18] Our first set of calculations were carried out on simple, minimalized models of the chromophore binding site (Figure 2). The Schiff base chromophore and the lysine side chain were included, and the chromophore was locked into a planar all-trans, 6-s-trans geometry. Aspartic acid side chains were simulated using CH_3-COO^- groups, the Arg-82 side chain by NH_4^+, and the divalent metal cation using Mg^{2+}. The model binding sites studied, labeled A−J, shown in Figure 2, represent a series of neutral and charged binding sites made up of various combinations of the chromophore, water, and positively or negatively charged counterions. In each case, the geometry was optimized with fixed intramolecular hydrogen bond lengths or metal-to-oxygen separations of 1.8 Å (dashed lines in Figure 2). The spectroscopic properties of these binding sites are summarized in Figures 3 and 4. Full protein binding site calculations were carried out on a subset of a more complete set of binding sites examined in ref 19. An MM2 calculation including the entire protein was carried out first, after assigning the local geometry of Arg-82 and, where applicable, Mg^{2+} (see Figures 5 and 6). The α-helical backbone atoms were fixed in all simulations to those based on electron cryomicroscopy data provided by Henderson and co-workers.[20] Following this optimization, a further minimization was carried out on the residues shown in Figures 5 and 6 using MNDO−PM3 theory. Excited-state calculations were carried out by using MNDO−PSDCI molecular orbital theory.[21−25] The CI basis set included all single and all double excitations, including triplet−triplet coupled doubles, from the π-electron system of the chromophore.[25] The MNDO−PSDCI spectroscopic parameters for Mg^{2+} are given in ref 19. The σ- and π-electron mobilities, m, were chosen on the recommendations of Zerner ($m_\sigma = 1.25$, $m_\pi = 0.585$).[26] The resulting over-correlation of the ground state was handled by multiplying the S_0 correlation energy by one-third prior to calculating the transition energies [see discussion in refs 25, 27, and 28].

Figure 3 (upper panel) shows the value calculated for the transition moment angle relative to the axis direction indicated in Figure 1, which runs from carbon-5 to carbon-15 for each of the 10 model cases shown in Figure 2. The lower solid symbols are for the "$1B_u^{*+}$" excitation, which is dominated by the π HOMO−LUMO singly excited configuration. The vertical position of the symbol and the number below it specifies the transition moment angle. The thickness of the symbol here (and in the lower panel) represents the calculated oscillator strength for the transition (also given numerically in the lower panel).

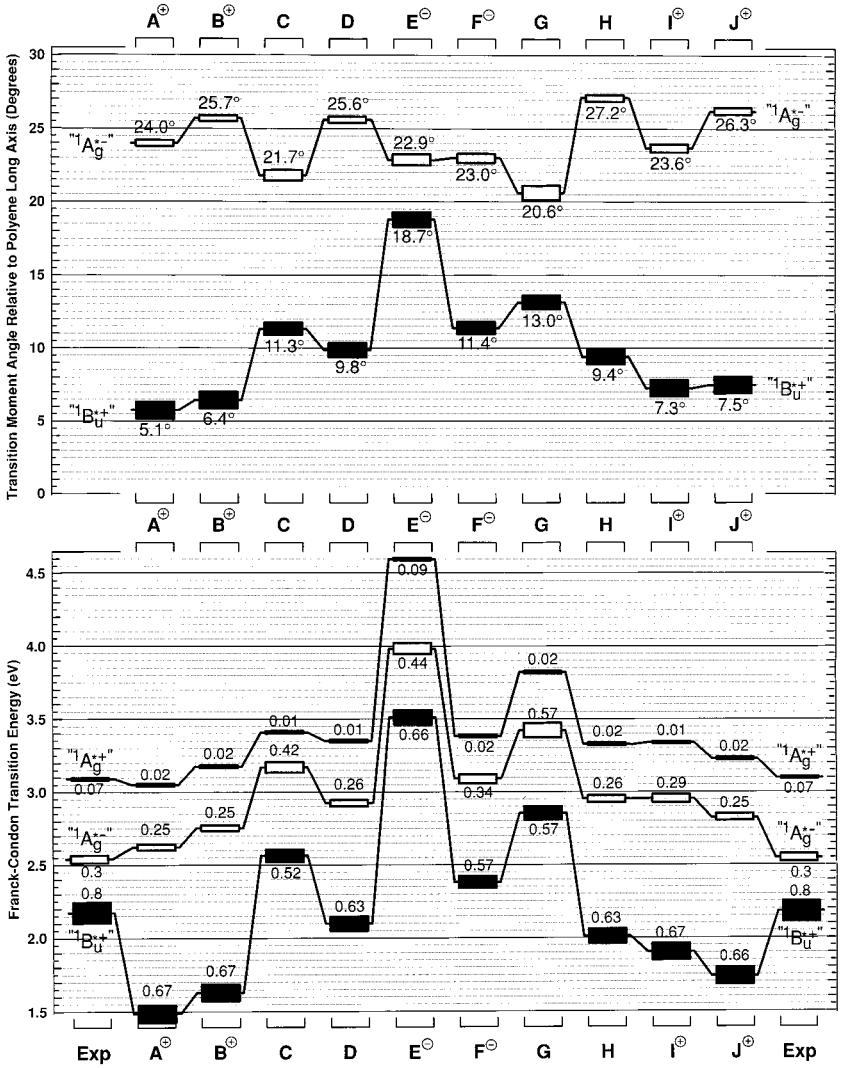

Figure 3. Excitation energies and transition dipole orientations of the model systems shown in Figure 2. The angle is defined with respect to a line drawn through atoms 5 and 15, as shown in Figures 1 and 6.

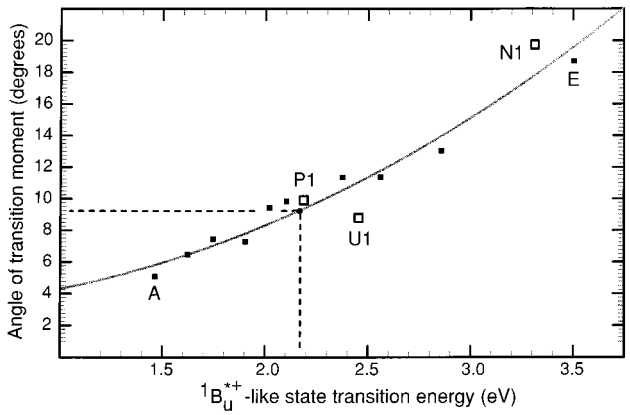

Figure 4. Correlation of the excitation energy and off-axis transition dipole orientation for the 10 models indicated in Figure 2 and the three protein binding site models indicated in Figure 5. The extreme cases of models A and E are indicated. The protein binding site models are also indicated and are labeled according to the legend for Figure 5. The dashed line is drawn at the excitation energy observed for bacteriorhodopsin.

The upper symbols in gray represent the same information for the "$1A_g^{*-}$" excitation dominated by doubly excited configurations. The significant intensity of this transition reflects the absence of inversion symmetry for these iminium model cases and significant mixing due to the large static dipole moment in the ground state.

The main point of this comparison is that the value of the off-axis direction varies considerably depending on the local binding site environment. The bare protonated retinal Schiff's base cation has the lowest value of only 5.1°, considerably smaller than the value calculated (13.5°) and observed (13.1°) for a conjugated hexaene.[11] The largest off-axis angle of 18.7° is observed for the model with two carboxylate anions directly neighboring the iminium nitrogen. The other negative or neutral models all give higher angles than the cation models. This pattern makes sense in terms of the effect of the bare iminium (model A) to result in a delocalized charge distributed over the π system and thus to have more nearly equal bond orders. The limiting case would be a cyanine dye that has, by symmetry, no off-axis component to its transition dipole orientation. The presence of negative or hydrogen bonding groups in the neighborhood of the iminium charge probably results in charge localization and (as seen in the lower panel) a blue shift of the electronic excitation energy for the "$1B_u^{*+}$" excitation toward the polyene value of 3.7 eV. Figure 4 shows that there is a strong correlation between the excitation energy and the off-axis angle for this excitation. Whatever the origin of this correlation, it suggests that models that give a reasonable excitation energy will give a finite off-axis angle.

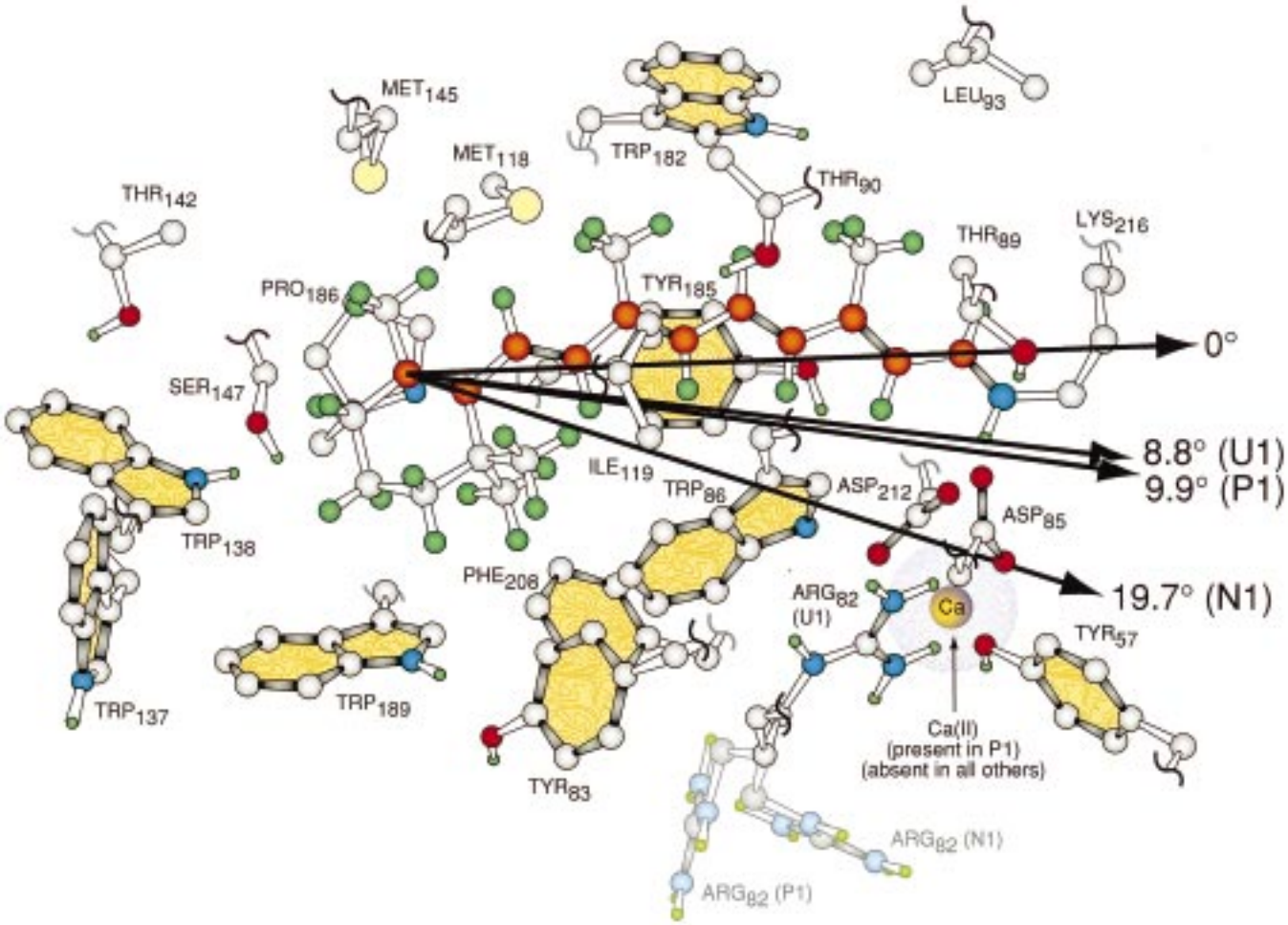

Figure 5. Basic molecular structure of the chromophore binding site along with the transition moment angles as a function of the charge on the binding site. The models examined are labeled N1 [negatively charged, Arg-82 down, no Ca(II)], U1 (neutral, Arg-82 up, no Ca(II)], and P1 [positively charged, Arg-82 down, Ca(II) as shown]. The transition moment angle is calculated relative to the chromophore polyene axis and is equal to 19.7° (N1), 8.8° (U1), or 9.9° (P1) and is thus dependent upon the nature of the binding site. However, we can rigorously rule out a negative binding site (N1), and thus the realistic range of values is 8.8°−9.9°, with the former value more likely based on analysis of the calculated spectroscopic properties (see ref 19). The MNDO calculations used Mg(II) in place of Ca(II) because the parameters were better defined for the former divalent metal cation, and experiments indicate that replacement of Ca(II) with Mg(II) has no observable impact on the spectroscopic properties of the light-adapted protein (see ref 24).

Clearly, the environment of the protonated Schiff base chromophore has a large effect on the off-axis angle. Just as the bare chromophore cannot be used to model the observed absorption maximum of 2.2 eV (left and right ends of the bottom panel), we do not expect it to provide a good model for the off-axis angle. Models that give approximately the right excitation energy (e.g., model D) give off-axis angles of 9°−10° (9.8° for model D). This is indicated in Figure 4.

It should be noted that the values of the angles given here refer to the specific model in vacuuo. There is a correction that must be applied in order to convert these values to the value expected in any condensed phase consisting of an elliptical cavity in a medium with some dielectric constant. This local field effect has been discussed previously[29] in a general context and has been applied in the context of the effect on apparent angle to the experimental determinations of the off-axis angle for simple polyenes[10,12−14] before making comparison to the corresponding theoretical (vacuum) values for those compounds.[11] The results are self-consistent, indicating that this elliptical cavity correction is accurate to within a half a degree or better. The magnitude of this elliptical cavity correction is about 5°, with the isolated molecule (vacuum) angle being smaller than the condensed phase value. Thus, a correction of this magnitude must be added to our calculated values unless the dispersive medium is explicitly included in the calculation. Our calculations include the dispersive medium only at the ground-state level, although overlap of the π system into neighboring residues is explicitly included in the CI calculations. To be conservative, therefore, we include the full range of possible corrections (0°−5°) in our final value and error estimate.

The origin of this angular correction factor derives from the fact that the presence of a dielectric medium external to the chromophore increases the electric field. If a chromophore is spherical, this external dielectric is excluded uniformly for all polarization directions. However, if the chromophore is elongated, the dielectric is more excluded and is less effective in enhancing the external field for electric fields parallel to the molecular long axis. If the electronic transition dipole is aligned along this long axis, this has no effect on the apparent polarization direction but only influences the apparent magnitude of the transition dipole moment. However, if the dipole is oriented at some angle with respect to the principal axes of the molecular elliptical cavity, the long and short axis components will be differently affected and the apparent angle will be changed.

We now turn to treatments of realistic models of the retinyl binding site of BR. These calculations are based on full binding sites that are partially illustrated in Figures 5 and 6. In these

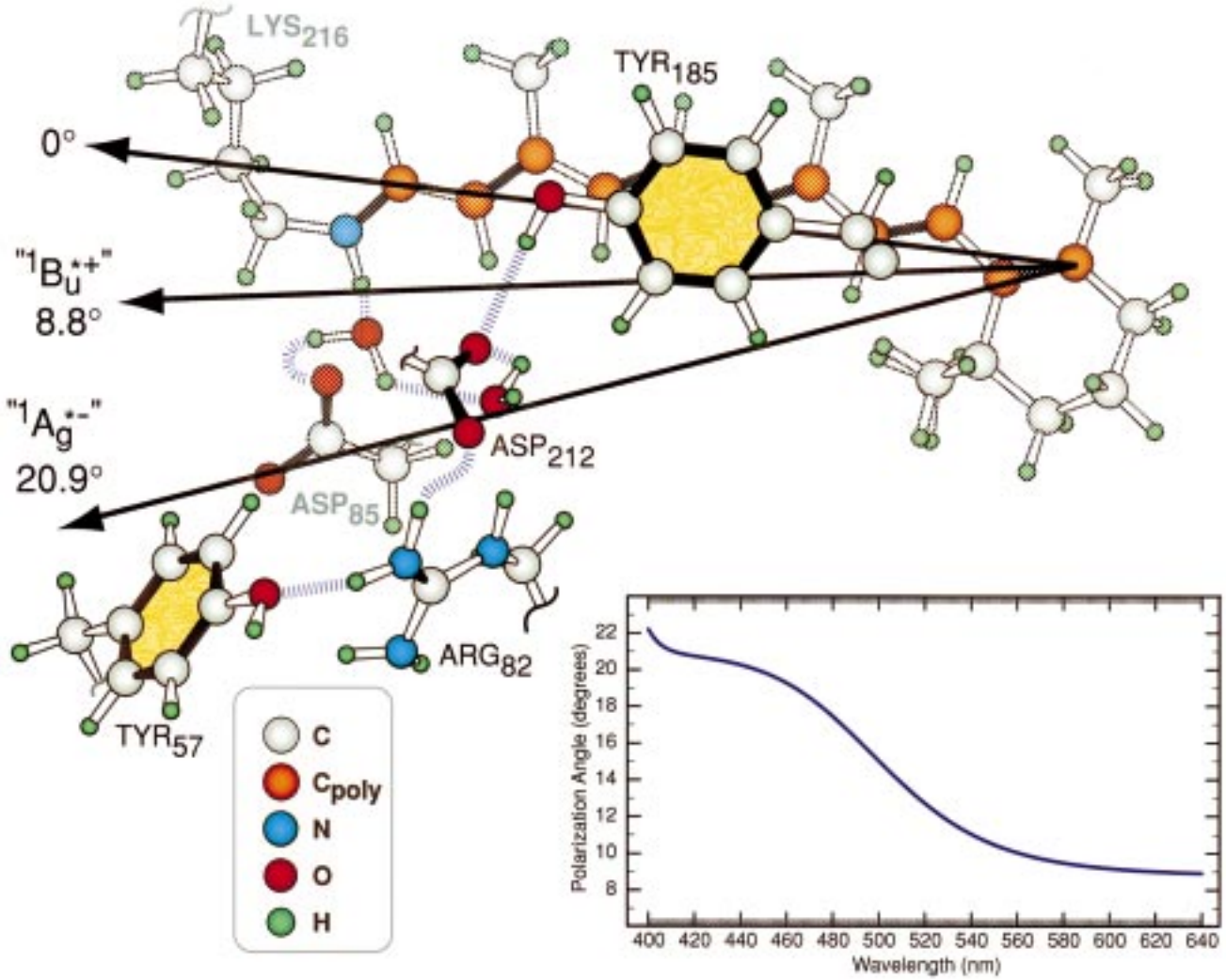

Figure 6. U1 binding site, a neutral chromophore binding site model that provides the best agreement with experiment based on an analysis of the one-photon and two-photon properties of light-adapted bacteriorhodopsin (see ref 19 for details). The lowest-lying $^1B_u{}^{*+}$-like state is calculated to have a transition moment of 8.8° relative to the chromophore polyene axis based on MNDO−CISD calculations. The excited $^1A_g{}^{*-}$-like state is calculated to have a transition moment of 20.9° relative to the chromophore polyene axis. By using the observed transition energies and bandwidths of these two states, we can estimate the effective transition moment angle as a function of the wavelength of excitation. The resulting dispersion is graphed at the lower right.

calculations, all of the residues and peptide backbone in contact with the chromophore are included in the MNDO−PSDCI calculation. Only chromophore $\pi \rightarrow \pi^*$ single and double excitations are included. The details of our models and our calculational procedures may be found in refs 19 and 21−24.

Figure 5 gives results for three different binding site models that have negative, neutral, and positive net charges in the binding pocket. In each case, there are two negatively charged aspartic acid residues close to the imine linkage of the protonated Schiff's base. With the side chain of arginine-82 in a distant position, the pocket is net negative. Movement of the arginine-82 side chain into the pocket makes it net neutral. Movement of the arginine away from the pocket and bonding of a Ca^{2+} ion makes it net positive. The resulting transition dipole angles are 19.7° (negative; N1), 8.8° (neutral; U1), and 9.9° (positive; P1). The angles, and the corresponding excitation energies, are consistent with the correlation found for the model systems as shown in Figure 4. Figure 6 gives additional information for one of these three binding site models, specifically the neutral U1 model. We choose this model for more detailed examination because it yields the best agreement with the one- and two-photon spectral data.[19] In addition to the transition dipole orientation of 8.8° for the "$1B_u{}^+$" excitation, the figure shows the orientation for the "$1A_g{}^{*-}$" transition of 20.9°. The "$1A_g{}^{*-}$" transition is calculated to be at a higher energy than the "$1B_u{}^{*+}$" transition and to have a relative oscillator strength that is approximately 40% of that of the "$1B_u{}^{*+}$" transition. This transition is expected to dominate in the blue tail of the absorption spectrum. This will result in an expected dispersion of the polarization angle as indicated in the inset to Figure 6. We concentrate here on the "$1B_u{}^{*+}$" transition because this transition dominates in the region of the optical dichroism studies.

This best overall fit model predicts that in the peak of the absorption spectrum and to the red of this region the off-axis transition moment will be on the order of 9°. This angle, however, refers to the results of such an experiment performed in vacuuo. (As noted above, our calculation does not include the dispersion interactions between the chromophore and nearby amino acids.) To make this condensed-phase correction, we use the method based on the considerations of ref 29 and the arguments as to the effective cavity shape and refractive index given in ref 30. Because of the very approximate nature of this local field cavity correction procedure and because of the gross

approximations utilized in its implementation (i.e., deciding what cavity dimension to use for the chromophore in the interior of the protein), we do not give the details of this calculation here but rather calculate extreme limits. Specifically, using the measured refractive index of BR films of 1.53,[30] we can calculate the effect of a cylindrical cavity of various axial ratios on the off-axis angle. Because the angle is near 0° the effect is small. One value of the ratio of the length to the diameter of the cavity is 2.5, as suggested by the analysis of ref 30. Just for the sake of argument, we also take a value that is twice as large, i.e., 5. The initial (vacuum) value of 8.8° then converts, in the first case, to a final value of 12.9° and, in the second case, to a value of 14.0°. Factors of two in the axial ratio result in changes of a degree in the angle. In this reasonable range, the magnitude of this effect is to increase the angle by 4°−5°. However, as noted below, a portion of the effects described by this field effect are included in the calculation. It is thus possible that no field adjustment should be applied to those values calculated for the full binding site. We thus include this possibility in assigning the error range of the correction factor.

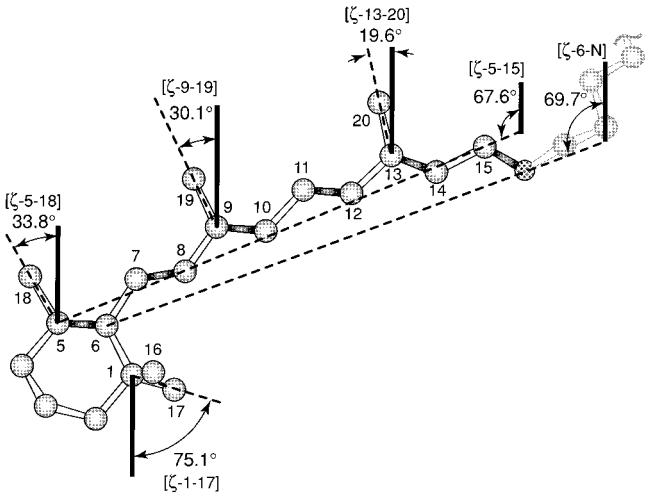

Figure 7. Structure of the chromophore as deduced from the 2.3 Å diffraction study of light-adapted bacteriorhodopsin by Luecke et al. (ref 33). The key angles for comparison with the optical dichroism and NMR studies are indicated.

Discussion

We now return to the structural issue at hand with reference to Figure 1. The calculations presented above indicate that there will be an off-axis angle for a reasonable model of the retinyl binding site of BR on the order of 10.8 ± 2.5°. This range is roughly that needed to reconcile the optical and ^{2}H NMR values within their respective errors. It should also be noted that various experiments have served to determine the orientation of the plane of the retinyl chromophore in terms of up versus down.[7] The proper orientation is as shown in Figure 1. Because of this orientation, the off-axis angle sense makes a difference; an angle of ∼10.5° in the other direction would increase rather than decrease the level of disagreement between theory and experiment.

Several arguments can be given to the effect that, whatever the inherent limitations of the quantum mechanical methods used, this estimate of the off-axis angle of 10.5 ± 3.5° is quite reliable. The first is that the same MNDO−PSDCI method, including the condensed-phase correction procedure, agrees (±0.4°) with the experimental values for simple linear polyenes where the experimental situation is unambiguous.[11] The second, relevant to the differences between retinal Schiff's base cations and simple polyenes, is that the correlation between the off-axis angle and the transition energy shown in Figure 4 for 10 simple protonated retinal Schiff's base/environment models plus the three binding site models strongly suggests that any model that yields the correct transition energy will generate approximately the same off-axis angle. This observation suggests that the details of the BR site are not critical in determining the off-axis angle so long as the result deduced from the proposed site has the correct transition energy. In other words, the angle is sensitive to the same factors as is the excitation energy. The variations of the condensed-phase corrections with axial ratio are so small that they can be neglected. The correction direction and magnitude (an *increase* of a few degrees) is certainly correct.

The last argument, off course, is that the conclusion of this investigation helps to reconcile the optical measurements with the ^{2}H NMR measurements. The resulting structure for the orientation of the chromophore and the orientation of its transition dipole (Figure 1) are roughly consistent within experimental error. Thus, the chromophore angle with optical dichroism results and standard deviation can now be adjusted to 61 ± 7°. The corresponding NMR results are 53.7 ± 4.1°. An evenly weighted reconciliation yields 57 ± 8°. The observed discrepancy is also consistent with the absolute orientation ("up" vs "down") and that the effect of flipping over the chromophore would be a discrepancy between these two methods of greater than 30°, well beyond the mutual limits of tolerance of the two methods. We note further that these calculations make the interesting prediction that the dichroism should exhibit dispersion as shown in the insert to Figure 6. This prediction appears to be in general agreement with the observations reported by Druckmann and Ottolenghi.[38]

After this paper was submitted, the atomic coordinates from the three recent diffraction studies were released.[31−33] These studies ranged in resolution from 2.3 to 2.8 Å, and all three studies observed electron density from the nonhydrogen atoms of the chromophore. The chromophore structure from the highest resolution study of Luecke et al.[33] is shown in Figure 7. Calculations on the properties of the binding site yielded results within a few percent of those calculated for our optimized structure shown in Figure 6. In addition to these diffraction coordinates, a new NMR study has been published providing an additional angular assignment of the chromophore β-ionylidene ring.[34] All of the NMR and diffraction results are compared in Table 1.

We find excellent agreement between the diffraction and NMR studies with respect to the angles measured on the β-ionylidine ring. For example, the angle of the C_5-C_{18} bond with the membrane normal is measured by NMR to be 37° (Figure 1, ref 3), and the average of the three recent diffraction studies is 38 ± 7° (Table 1). Similarly, the angle of the C_1-C_{17} bond with the membrane normal is measured by NMR to be 68.7 ± 2° (ref 34), and the average of the three recent diffraction studies is 72 ± 5° (Table 1). In contrast, the angles measured for the C_{19} and C_{20} methyl groups by the two methods differ significantly (Table 1). Because these angles are of significant importance in assigning the total angular orientation of the chromophore, there is a significant difference between the NMR chromophore angle ($\Omega = 53.7 \pm 4.1°$) and the average value deduced from the diffraction data ($\Omega = 70.6 \pm 3.2°$). This discrepancy between the two methods for angles near the imine nitrogen has been noted before, and it has been suggested that the diffraction studies are contaminated by the presence of 13-cis,15-syn dark-adapted species.[34] This view is not unreasonable given the difficulty of fully light-adapting a crystalline matrix.[6] An additional source of discrepancy between the two

TABLE 1: Bacteriorhodopsin Chromophore Orientation Relative to Membrane Normal as Determined by NMR and Diffraction Studies

angle[a]	deuterium NMR[b,c]	angles based on diffraction studies				
		ref 20[d]	ref 31[e]	ref 32[f]	ref 33[g]	av[h]
			Methyls			
[ζ−1-17]	68.7 ± 2°[c]	67.4°	66.4°	74.7°	75.1°	72 ± 5°
[ζ−5-18]	37°	38.6°	45.2°	33.8°	33.8°	38 ± 7°
[ζ−9-19]	40°	29.2°	37.9°	39.2°	30.1°	36 ± 5°
[ζ−13-20]	32°	16.1°	9.4°	16.7°	19.6°	15 ± 5°
			Polyene			
$\Omega(\langle^{\perp}_{C-Me})^i$	53.7 ± 4.1°	62.0°	59.2°	60.1°	62.2°	60.5 ± 1.5°
Ω [ζ−5-15][j]		70.7°	70.3°	74.0°	67.6°	70.6 ± 3.2°

[a] The angles relative to the membrane normal are defined in Figure 7. [b] All data from ref 3 unless noted otherwise. [c] Datum from ref 34. [d] Angles relative to the *z* axis with coordinate data from PDB file kindly provided by Richard Henderson.[20] [e] Angles relative to the *z* axis with coordinate data from Brookhaven PDB file: 1AP9.[31] [f] Angles relative to the *z* axis with coordinate data from Brookhaven PDB file: 1AT9.[32] [g] Angles relative to the *z* axis with coordinate data from PDB file 1BRX kindly provided by Janos Lanyi.[33] These angles are shown in Figure 7. [h] Average of the angles derived from the three recent diffraction studies, all of which resolve the chromophore electron density (refs 31−33). [i] Chromophore angle based on the assumption that the polyene chain is perpendicular to the methyl group bonds: $\Omega(\langle^{\perp}_{C-Me}) = 90° - (1/3)([\zeta\text{-}5\text{-}18] + [\zeta\text{-}9\text{-}19] + [\zeta\text{-}13\text{-}20])$. [j] Chromophore angle based on a line drawn through atoms C_5 and C_{15} (see Figure 1). This is the definition used in deriving our correction for the optical dichroism data.

methods is due to the procedure of calculating the chromophore angle. The NMR study[3] calculated the value of Ω by using the following relationship:

$$\Omega(\langle^{\perp}_{C-Me}) = 90° - \frac{1}{3}([\zeta\text{-}5\text{-}18] + [\zeta\text{-}9\text{-}19] + [\zeta\text{-}13\text{-}20]) \quad (1)$$

which is based on the assumption that the chromophore angle is perpendicular to the methyl group bonds. This assumption is reasonable for a polyene chromophore that is not bent. The highest resolution diffraction measurement[33] suggests rather significant bending of the chromophore, and thus the methyl group angles diminish systematically in moving from the *β*-ionylidene ring toward the imine nitrogen (Figure 7). Indeed, if we use eq 1 to calculate the chromophore angle based on the diffraction coordinates, we get an average value in much better agreement with the NMR results (Ω = 60.5 ± 1.5°, Table 1). It should also be noted that a structure obtained with a resolution of ∼2.5 Å would allow for angular ranges for the entire chromophore of about 8° and local angular ranges as large as 20°. However, the observation that all three of the recent diffraction studies yield a total chromophore angle of Ω = 70.6 ± 3.2° suggests a surprising level of agreement given the resolution. In summary, the diffraction result is in agreement with the revised optical dichroism result (Ω = 61 ± 7°) but is not within reach of the NMR result (Ω = 53.7 ± 4.1°). Further experimental work will be required to resolve this discrepancy.

In closing, we examine a more general result that concerns the relevance of model compounds such as retinal to the transition moment of the protonated retinyl Schiff's base chromophore. The crystal dichroism results for retinal[35] have been used in some analyses of rhodopsin dichroism studies[36,37] and have been noted in some studies of bacteriorhodopsin. Figure 8a gives the results of calculations of the off-axis angle for retinal, the unprotonated Schiff's bases, and the protonated Schiff's base with no counterion for two different conformations of the 6−7 bond. (It is interesting to note that the conformational effect on the "$^1B_u{}^{*+}$" transition moment is consistently 3.4 ± 0.1°.) The calculated "$^1B_u{}^{*+}$" transition angle value is quite different for these three species. It is thus fortuitous that the value for the protonated Schiff's base when the counterion and environment are included (8.8°, Figure 6) differs from that of retinal by only 3°. It is clear, however, that the use of dichroism to analyze chromophore orientation must take into account the protonation state of the chromophore as well as the transition energy. The latter variable is important even for studies of the same chromophore in changing protein environments (Figure 5). In general, all of the effects, whether associated with environment or chromophore protonation state, appear to scale roughly as a function of the transition energy (Figures 4 and 8b). We alluded to this possibility before in discussing Figure 4, but the examples shown in Figure 8a provide a more structurally varied sample and yield the same observation. When dichroism is used to deduce chromophore angle, we suggest that a correction for the effect of transition energy on the transition moment angle be included. The following formula provides a best fit of the transition moment of the strongly allowed "$^1B_u{}^{*+}$" state relative to the chromophore polyene axis for all of the systems studied here:

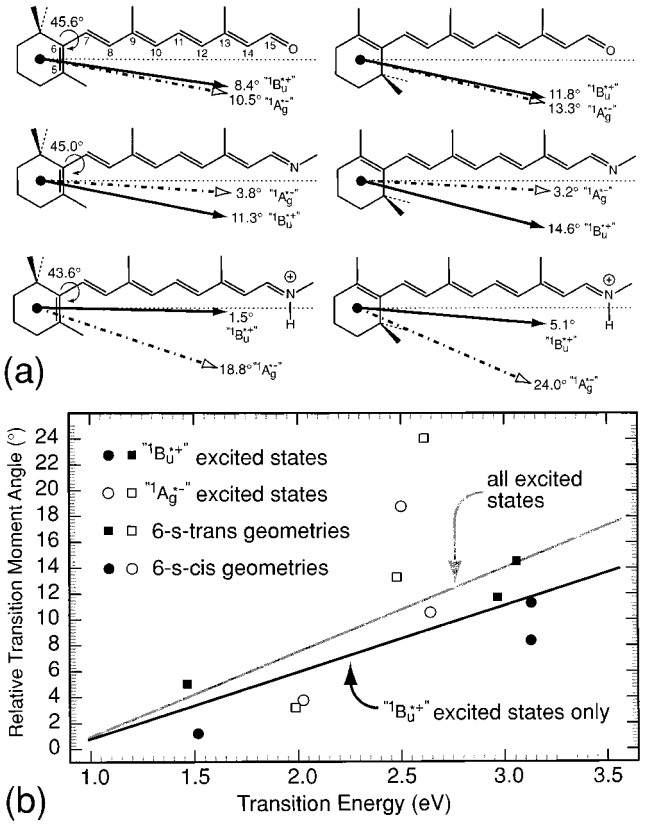

Figure 8. Calculated transition dipole orientations for selected retinal isomers and derivatives based on the MNDO−PSDCI method. In calculations involving 6-s-cis species, the angle is calculated relative to a line connecting atoms C_6 and the carbonyl oxygen or imine nitrogen atom. The graph in insert (b) shows the effect of transition energy on the transition moment angle for the set of molecules shown in (a). The resulting fit displays a slope and intercept very similar to that observed in Figure 4 for the model protonated Schiff base chromophores.

$$\theta = 2.246°\left(\frac{1240\text{ nm}}{\lambda_{max}}\right) + 0.7846°\left(\frac{1240\text{ nm}}{\lambda_{max}}\right)^2 \quad (350\text{ nm} < \lambda_{max} < 700\text{ nm}) \quad (2)$$

This equation will typically underestimate the transition moment angle for polyenes and can be viewed as a gentle (rather than

aggressive) correction factor. In that regard, it does not include contributions from higher lying excited states nor the cavity field correction discussed above. Both factors will tend to increase the angle by about 4°−5° for an all-trans retinyl polyene.

Acknowledgment. This work was supported in part by grants from NIH (GM-34548), NSF (CHE-9503629), and the W. M. Keck Foundation. The authors thank Drs. Tony Watts and David Kliger for interesting and helpful discussions and Drs. Richard Henderson and Janos Lanyi for providing us with the coordinates from their diffraction studies.

References and Notes

(1) Ulrich, A. S.; Watts, A.; Wallat, I.; Heyn, M. P. Distorted Structure of the Retinal Chromophore in Bacteriorhodopsin Resolved by ^{2}H NMR. *Biochemistry* **1994**, *33*, 5370.

(2) Ulrich, A. S.; Heyn, M. P.; Watts, A. Structure Determination of the Cyclohexene Ring of Retinal in Bacteriorhodopsin by Solid-State Deuterium NMR. *Biochemistry* **1992**, *31*, 10390.

(3) Watts, A.; Ulrich, A. S.; Middletown, D. A. Membrane protein structure: The contributions and potential of novel solid-state NMR approaches. *Membr. Mol. Biol*. **1995**, *12*, 233.

(4) Heyn, M. P.; Cherry, R. J.; Müller, U. Transient and Linear Dichroism Studies on Bacteriorhodopsin: Determination of the Orientation of the 568 nm All-trans Retinal Chromophore. *J. Mol. Biol*. **1977**, *117*, 607.

(5) Barabas, K.; Der, A.; Dancshazy, Zs.; Ormos, P.; Keszthelli, L.; Marden, M. Electrooptical measurements on Aqueous Syspension of Purple Membrane from Halobacterium Halobium. *Biophys. J.* **1983**, *43*, 5.

(6) Schertler, G. F. X.; Lozier, R.; Michel, H.; Oesterhelt, D. Chromophore motion during the bacteriorhodopsin photocycle: polarized absorption spectroscopy of bacteriorhodopsin and its M-state in bacteriorhodopsin crystals. *EMBO J.* **1991**, *10*, 2353.

(7) Lin, S. W.; Mathies, R. A. Orientation of the protonated retinal Schiff base group in bacteriorhodopsin from absorption linear dichroism. *Biophys. J.* **1989**, *56*, 653.

(8) Fahmy, K.; Siebert, F.; Tavan, P. Structural investigation of bacteriorhodopsin and some of its photoproducts by polarized Fourier transform infrared spectroscopic methods-difference spectroscopy and photoselection. *Biophys. J.* **1991**, *60*, 989.

(9) Earnest, T. N.; Roepe, P.; Braiman, M. S.; Gillespie, J.; Rothschild, K. J. Orientation of the Bacteriorhodopsin Chromophore Proben by Polarized Fourier Transform Infrared Difference Spectroscopy. *Biochemistry* **1986**, *25*, 7793.

(10) Shang, Q.-Y.; Dou, X.; Hudson, B. S. Off-axis orientation of the electronic transition moment for a linear conjugated polyene. *Nature* **1991**, *352*, 703.

(11) Birge, R. R.; Zgierski, M. Z.; Serrano-Andres, L.; Hudson, B. S. The Transition Dipole Orientation of Linear Polyenes: Semiempirical Models and Extrapolation to the Infinite Chain Limit. *J. Phys. Chem. A* **1999**, *103*, 2251.

(12) Dou, X.; Shang, Q.-Y.; Hudson, B. S. Analysis of the decay of the fluorescence anisotropy of 2,4,6,8-decatetraene in a viscous hydrocarbon solution: the off-axis orientation of the transition dipole moment. *Chem. Phys. Lett*. **1992**, *189*, 48.

(13) Lee, K. S.; Shang, Q.-Y.; Hudson, B. S. Urea and thiourea inclusion crystals of conjugated polyenes: polarized fluorescence excitation and resonance Raman studies. *Mol. Cryst. Liq. Cryst*. **1992**, *211*, 147.

(14) Shang, Q.-y. Ph.D. Thesis, University of Oregon, 1990.

(15) Dewar, M. J. S.; Thiel, W. Ground states of molecules. 38. The MNDO method. Approximations and parameters. *J. Am. Chem. Soc*. **1977**, *99*, 4899.

(16) Dewar, M. J. S.; Zoebisch, E. G.; Healy, E. F.; Stewart, J. J. P. AM1: A new general purpose quantum mechanical molecular model. *J. Am. Chem. Soc*. **1985**, *107*, 3902−3909.

(17) Stewart, J. J. P. Optimization of parameters for semiempirical methods. *J. Comput. Chem.* **1989**, *10*, 221.

(18) Thiel, W. Semiempirical methods: Current status and perspectives. *Tetrahedron* **1988**, *44*, 7393.

(19) Kusnetzow, A.; Singh, D. L.; Martin, C. H.; Barani, I.; Birge, R. R. Nature of the Chromophore Binding Site of Bacteriorhodopsin. The Potential Role of Arg-82 as a Principal Counterion. *Biophys. J*., in press.

(20) Grigorieff, N.; Ceska, T. A.; Downing, K. H.; Baldwin, J. M.; Henderson, R. Electron-crystallographic refinement of the structure of bacteriorhodopsin. *J. Mol. Biol.* **1996**, *259*, 393.

(21) Tallent, J. R.; Hyde, E. Q.; Findsen, L. A.; Fox, G. C.; Birge, R. R. Molecular dynamics of the primary photochemical event in rhodopsin. *J. Am. Chem. Soc*. **1992**, *114*, 1581.

(22) Tallent, J. R.; Birge, J. R.; Zhang, C. F.; Wenderholm, E.; Birge, R. R. Conformational energetics and excited-state level ordering in 11-cis retinal. *Photochem. Photobiol*. **1992**, *56*, 935.

(23) Birge, R. R.; Gross, R. B.; Masthay, M. B.; Stuart, J. A.; Tallent, J. R.; Zhang, C. F. Nonlinear optical properties of bacteriorhodopsin and protein based two-photon three-dimensional memories. *Mol. Cryst. Liq. Cryst. Sci. Technol., Sect. B.* **1992**, *3*, 133.

(24) Stuart, J. A.; Vought, B. W.; Zhang, C. F.; Birge, R. R. The active site of bacteriorhodopsin. Two-photon spectroscopic evidence for a positively charged chromophore binding site mediated by calcium. *Biospectrosc.* **1995**, *1*, 9.

(25) Martin, C. H.; Birge, R. R. Reparametrizing MNDO for excited-state calculations using ab initio effective Hamiltonian theory: Application to the 2,4-pentadien-1-iminium cation. *J. Phys. Chem. A* **1998**, *102*, 852.

(26) Zerner, M. C. Semiempirical molecular orbital methods. In *Reviews in Computational Chemistry*; Lipkowitz, K. B., Boyd, D. B., Eds.; VCH Publishers: New York, 1990; p 313.

(27) Birge, R. R.; Schulten, K.; Karplus, M. Possible influences of a low-lying 'covalent' excited state on the absorption spectrum and photoisomerization of 11-cis retinal. *Chem. Phys. Lett*. **1975**, *31*, 451.

(28) Schulten, K.; Ohmine, J.; Karplus, M. Correlation effects in the spectra of polyenes. *J. Chem. Phys.* **1976**, *64*, 4422.

(29) Myers, A. B.; Birge, R. R. The effect of solvent environments on molecular electronic oscillator strengths. *J. Chem. Phys*. **1980**, *73*, 5314.

(30) Yamazaki, M.; Goodisman, J.; Birge, R. R. Quadratic electrooptic effects in bacteriorhodopsin: Measurement of $\gamma(-\omega; 0, 0,\omega)$ in dried gelatin thin films. *J. Chem. Phys*. **1998**, *108*, 5876.

(31) Pebay-Peyroula, E.; Rummel, G.; Rosenbusch, J. P.; Landau, E. M. X-ray structure of bacteriorhodopsin at 2.5 Å from microcrystals grown in lipidic cubic phases. *Science* **1997**, *277*, 1676−1681.

(32) Kimura, Y.; Vassylyev, D. G.; Miyazawa, A.; Kidera, A.; Matsushima, M.; Mitsuoka, K.; Murata, K.; Hirai, T.; Fujiyoshi, Y. Surface of bacteriorhodopsin revealed by high-resolution electron cyrstallography. *Nature* **1997**, *389*, 206−211.

(33) Luecke, H.; Richter, H. T.; Lanyi, J. K. Proton-transfer pathways in bacteriorhodopsin at 2.3 Angstrom resolution. *Science* **1998**, *280*, 1934−1937.

(34) Moltke, S.; Nevzorov, A. A.; Sakai, N.; Wallat, I.; Job, C.; Nakanishi, K.; Heyn, M. P.; Brown, M. F. Chromophore Orientation in Bacteriorhodopsin Determined from the Angular Depencdence of Deuterium Nuclear Magnetic Resonance Spectra of Oriented Purple Membranses. *Biochemistry* **1998**, *37*, 11821.

(35) Drikos, G.; Ruppel, H.; Sperling, W.; Morys, P. Polarized UV-absorption spectra of retinal isomers- I measurements in extremely thin monochrystal plates. *Photochem. Photobiol.* **1984**, *40*, 85. Drikos, G.; Ruppel, H. Polarized UV-absorption spectra of retinal isomers − II on the assignment of the low and high energy absorption bands. *Photochem. Photobiol*. **1984**, *40*, 93.

(36) Lewis, J. W.; Einterz, C. M.; Hug, S. J.; Kliger, D. S. Transition dipole orientations in the early photolysis intermediates of rhodopsin. *Biophys. J*. **1989**, *56*, 1101.

(37) Jager, S.; Lewis, J. W.; Zvyaga, T. A.; Szundi, I.; Sakmar, T. P. Chromophore structural changes in rhodopsin from nanoseconds to microseconds following pigment photolysis. *Proc. Natl. Acad. Sci.* **1997**, *94*, 8557.

(38) Druckmann, S.; Ottolenghi, M. Electric dichroism in the purple membrane of Halobacterium halobium. *Biophys. J.* **1981**, *33*, 263.